CHINESE OPTICS LETTERS

Vol. 21, No. 3 | March 2023

Continuous-wave three-wavelength operation of a diode-pumped Tm:YVO_4 laser on the $^3H_4 \rightarrow {}^3H_5$ and $^3F_4 \rightarrow {}^3H_6$ transitions

Jiaqun Zhao (赵家群)[1*], Yuantong Liu (刘原彤)[1], Ping Cheng (成 萍)[2], and Rui Yu (俞 瑞)[1]

[1] College of Science, Hohai University, Nanjing 211100, China

[2] College of Computer and Information, Hohai University, Nanjing 211100, China

*Corresponding author: zhaojq@hhu.edu.cn

Received March 24, 2022 | Accepted September 20, 2022 | Posted Online November 3, 2022

A diode-pumped continuous-wave Tm:YVO_4 laser operating on the $^3H_4 \rightarrow {}^3H_5$ and $^3F_4 \rightarrow {}^3H_6$ transitions was demonstrated for the first time, to the best of our knowledge. An a-cut Tm:YVO_4 crystal with 1.5% (atomic fraction) Tm^{3+} ion concentration was used to characterize the laser behavior. A common commercial laser diode with a central wavelength of 790 nm and a bandwidth of 3.2 nm was utilized as a pump source. With an output coupler for the $^3H_4 \rightarrow {}^3H_5$ and $^3F_4 \rightarrow {}^3H_6$ transitions, simultaneous three-wavelength laser operation was achieved. The laser emissions at 2292 and 2363 nm in π-polarization and at 2108 nm in σ-polarization were realized. With an incident pump power of 22 W, the total output power of 1.17 W at 2292, 2363, and 2108 nm was obtained. The output power at 2292 and 2363 nm was measured to be 750 mW, and the output power at 2108 nm was measured to be 420 mW.

Keywords: Tm:YVO_4 crystal; three-wavelength; $^3H_4 \rightarrow {}^3H_5$ transition.

DOI: 10.3788/COL202321.031401

1. Introduction

Mid-infrared laser sources emitting in the 2–2.5 μm special region have attracted a great deal of interest in recent years. Such emission falls in the atmospheric transparency window. Some important gas molecules such as N_2O (2.28 μm), CO (2.3 μm), CH_4 (2.35 μm), NH_3 (2.1 μm), and HF (2.5 μm), exhibit strong absorption lines in this region. Especially, 2.3 μm lasers have been applied to gas sensing in the atmosphere[1,2] and noninvasive blood glucose measurements[3,4]. Various approaches have been used to obtain 2.3 μm laser emission. A solid-state Raman laser based on stimulated Raman scattering (SRS) can produce 2.3 μm laser emission[5]. Semiconductor lasers operating near 2.3 μm have been reported[6]. Cr^{2+}:ZnS and Cr^{2+}:ZnSe lasers have also directly generated laser emissions in the special region[7,8].

A promising approach to generate 2.3 μm laser emission is using the $^3H_4 \rightarrow {}^3H_5$ quasi-four-level transition of the Tm^{3+} ions in a host crystal. The energy-level scheme of Tm^{3+} ions in a host crystal is shown in Fig. 1. In the early 1970s, 2.3 μm laser emission based on the prediction of the Judd–Ofelt theory was realized in Tm-doped oxide host materials[9]. By now, lasers at 2.3 μm based on the Tm^{3+} $^3H_4 \rightarrow {}^3H_5$ transition have been reported and analyzed theoretically in various host crystals, e.g., Tm:YAG[9,10], Tm:YAP[9,11–14], Tm:YLF[13,15–18], Tm:KYF[19–21], Tm:LuAG[22], and Tm:Klu$(WO)_4$[23]. These lasers based on the Tm^{3+} $^3H_4 \rightarrow {}^3H_5$ transition in different host crystals can generate laser emissions with different wavelengths. Among the studies, Tm:YLF and Tm:YAP lasers with relatively low Tm^{3+} ion concentration were mainly demonstrated. Narrow-linewidth high-quality Ti:sapphire lasers were commonly used as pump sources to pump 2.3 μm Tm lasers[11,18–21]. Recently, diode-pumped 2.3 μm Tm lasers have been reported[12,17].

So far, continuous-wave (CW) 2.3 μm Tm lasers have also been reported by several groups. For example, Wang *et al.* reported an a-cut Tm:YAP laser generating a maximum CW output power of 1.12 W at dual-wavelength of 2274 and 2383 nm with a slope efficiency of 14.0%[12]. Guillemot *et al.* reported a CW Tm:YAG laser delivering a maximum output power of 1.07 W at 2.19 and 2.32 μm with a slope efficiency of 46.3%[10]. Muti *et al.* demonstrated a Tm:KYF laser operating at 2.34 μm and generating 0.12 W with a slope efficiency of 18%[19]. Loiko *et al.* reported a diode-pumped quasi-CW Tm:$LiYF_4$ laser delivering a maximum peak output power of 2.4 W at 2306 nm with a slope efficiency of 11.5%[24].

However, to our knowledge, laser emission on the $^3H_4 \rightarrow {}^3H_5$ transition in Tm-doped vanadate crystals has not been reported.

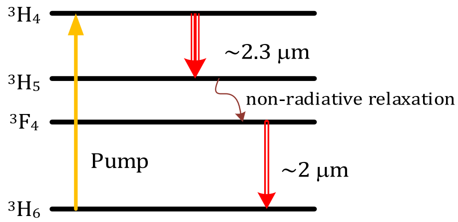

Fig. 1. Energy-level scheme of Tm^{3+} ions in host crystal.

So far, studies on Tm-doped vanadate (e.g., $Tm:YVO_4$[25–28], $Tm:GdVO_4$[27–29], and $Tm:LuVO_4$[27,28]) lasers have mainly focused on the $^3F_4 \rightarrow {}^3H_6$ transition around 1.9 μm. Among the vanadate crystals, the $Tm:YVO_4$ crystal with natural birefringence is an excellent laser gain medium for 1.9 μm laser due to its large absorption and emission cross sections. For the $Tm:YVO_4$ crystal, the calculated lifetimes of $^3F_4$, $^3H_5$, and $^3H_4$ excited states were 1208, 1237, and 224 μs, and the measured lifetimes of $^3F_4$ and $^3H_4$ were 1.9 ms and 176 μs, respectively[30]. For the $^3H_6 \rightarrow {}^3H_4$ transition of the $Tm:YVO_4$ crystal, the peak absorption cross section for π polarization reached 2.8×10^{-20} cm^2 near 800 nm, and the peak stimulated emission cross section corresponding to the $^3F_4 \rightarrow {}^3H_6$ transition was close to 2.8×10^{-20} cm^2[30]. The strong absorption in $Tm:YVO_4$ should make it more suitable for microchip lasers. Zayhowski *et al.* reported a 5% (atomic fraction) $Tm:YVO_4$ microchip laser producing an output power of 150 mW at 1.92 μm with a slope efficiency of 20%[31]. Saito *et al.* demonstrated a room-temperature 5% $Tm:YVO_4$ laser obtaining an output power of 48 mW at 1.94 μm with a slope efficiency of 25%[26]. Hu *et al.* reported a 3% $Tm:YVO_4$ laser producing a maximum CW output power of 2.59 W at 1923.1 nm with a slope efficiency of 41.7%[25].

The main goal of the work described here is to report laser emission on the $^3H_4 \rightarrow {}^3H_5$ transition at 2.3 μm in a $Tm:YVO_4$ crystal. In this study, to the best of our knowledge, we demonstrated a diode-pumped CW $Tm:YVO_4$ laser simultaneously operating on the $^3H_4 \rightarrow {}^3H_5$ and $^3F_4 \rightarrow {}^3H_6$ transitions for the first time. A common commercial laser diode (LD) with a central wavelength of 790 nm was used as a pump laser source. A simple linear resonant cavity was adopted. With an output coupler for the $^3H_4 \rightarrow {}^3H_5$ and $^3F_4 \rightarrow {}^3H_6$ transitions, the output powers of 750 mW at 2292 and 2363 nm and 420 mW at 2108 nm were obtained at the same time.

2. Experimental Design

The scheme of a diode-pumped $Tm:YVO_4$ laser is shown in Fig. 2. A common commercial fiber-coupled LD was used as a pump source, and the maximum output pump power was 22 W. The output-coupling fiber of the LD had a core diameter of 400 μm and a numerical aperture (N.A.) of 0.22. The central wavelength of the LD was measured to be 790 nm at 25°C. The full width at half-maximum (FWHM) of the LD was about 3.2 nm. The pump beam from the output-coupling fiber was coupled into the $Tm:YVO_4$ crystal by two identical plano–convex lenses with focal lengths of 25 mm and high transmission at 780–810 nm. The waist radius of the pump beam within the laser crystal was estimated to be 200 μm. The pump light from the LD operating in the CW regime was unpolarized. The uncoated *a*-cut $Tm:YVO_4$ crystal with 1.5% Tm^{3+} ion concentration was used as laser gain medium. Tm^{3+} ion concentration around 1.5% contributed to efficient laser emission on the $^3H_4 \rightarrow {}^3H_5$ transition in Tm-doped crystals[22]. The end faces of the $Tm:YVO_4$ crystal with the dimension of 3 mm × 3 mm × 20 mm were parallel. The $Tm:YVO_4$ crystal was wrapped with indium foil and mounted in a water-cooled copper heat sink. The heat sink temperature was controlled by a thermoelectric cooler system.

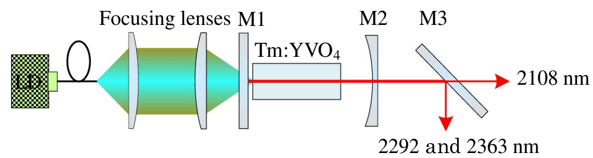

Fig. 2. Scheme of a $Tm:YVO_4$ laser operating on the $^3H_4 \rightarrow {}^3H_5$ and $^3F_4 \rightarrow {}^3H_6$ transitions.

The simple linear resonant cavity was composed of an input mirror (M1) and an output coupler (M2). M1 was a flat input mirror, which was designed to be high-transmittance coated at 780–810 nm and high-reflection coated at 1900–2400 nm ($R > 99.8\%$). M2 was a plano–concave output coupler with a curvature radius of 100 mm, which was designed to partial reflection at 1900–2150 nm ($R = 95\%$) and partial reflection at 2250–2400 nm ($R = 99\%$) to realize laser emissions on the $^3H_4 \rightarrow {}^3H_5$ and $^3F_4 \rightarrow {}^3H_6$ transitions simultaneously. Both of the cavity mirrors were made of CaF_2. The physical cavity length was about 30 mm. A 45° flat dichroic mirror (M3) coated for high transmissivity at 2108 nm ($T > 95\%$) and high reflectivity at 2292 and 2663 nm ($R > 98\%$) was used to separate the laser emissions on the $^3H_4 \rightarrow {}^3H_5$ and $^3F_4 \rightarrow {}^3H_6$ transitions.

3. Experimental Results and Discussion

The feasibility of achieving laser emissions on the $^3H_4 \rightarrow {}^3H_5$ and $^3F_4 \rightarrow {}^3H_6$ transitions in the $Tm:YVO_4$ crystal was studied. With the output coupler coated for partial reflection at 1900–2150 nm ($R = 95\%$) and partial reflection at 2250–2400 nm ($R = 99\%$), a three-wavelength $Tm:YVO_4$ laser can be realized. Figure 3 shows the spectral information of the $Tm:YVO_4$ laser, which was recorded at the maximum incident pump power of 22 W. Three spectral lines with central wavelengths of 2108, 2292, and 2363 nm were observed. The corresponding FWHMs of the three output wavelengths were about 14.5, 8.4, and 9.3 nm, respectively. The three output central wavelengths were almost unchanged when the incident power was different. The lasing spectrum was measured by a commercial grating monochromator (Zolix, Omni-λ3007) with a resolution of 0.1 nm. The two

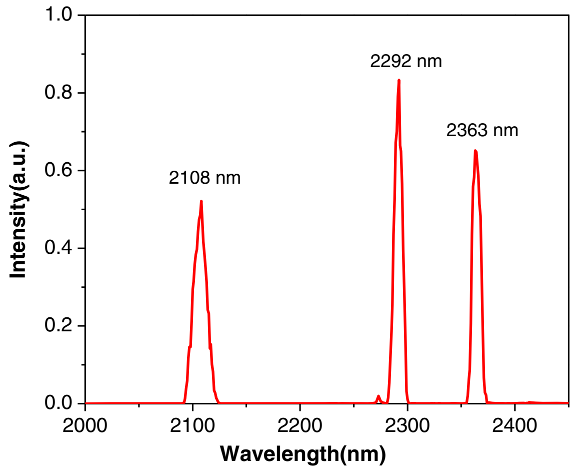

Fig. 3. Lasing spectrum of the Tm:YVO_4 laser.

spectral lines of 2292 and 2363 nm corresponded to the $^3H_4 \rightarrow {}^3H_5$ transition. The multiwavelength behavior on the $^3H_4 \rightarrow {}^3H_5$ transition could be caused by the transitions between the Stark components of the $^3H_4 \rightarrow {}^3H_5$ multiplets[23,30].

In this experiment, the output powers and pump power were measured by a power meter (Coherent, PM30). The absorbed pump power of the Tm:YVO_4 crystal can be measured by removing the mirrors M2 and M3, and the absorbed pump efficiency of the crystal was calculated to be around 92.5%. The output powers of the Tm:YVO_4 laser were measured as a function of incident pump power; the results are plotted in Figs. 4 and 5. Heat sink temperature affected the oscillation threshold and output powers of the Tm:YVO_4 laser. At a heat sink temperature of 20°C, the pump threshold of the Tm:YVO_4 laser was about 11.7 W, and the maximum total output power was 802 mW. When the heat sink temperature was controlled at 12°C, the pump threshold power decreased to 9.8 W, and the maximum total output power increased to 1170 mW. Figure 4 shows that low heat sink temperature was beneficial to reduce pump threshold and enhance conversion efficiency.

As seen in Fig. 5, the laser emissions on the $^3H_4 \rightarrow {}^3H_5$ and $^3F_4 \rightarrow {}^3H_6$ transitions had different pump thresholds. When incident pump power was 9.8 W, a laser spectral line of 2363 nm was observed. A spectral line of 2292 nm was also observed when the incident pump power was increased to 10.5 W. When incident pump power was increased to 11.7 W, a spectral line of 2108 nm appeared. At the maximum incident pump power of 22 W, the Tm:YVO_4 laser generated a total output power of 1.17 W for the three wavelengths with an optical-to-optical conversion efficiency of 5.3% and a slope efficiency of 10.4% (both calculated relative to the incident pump power). The maximum output power at 2108 nm was measured to be 420 mW. To our knowledge, this is the first time laser emission of the Tm:YVO_4 laser on the $^3F_4 \rightarrow {}^3H_6$ transition beyond 2.1 μm has been obtained. The maximum output power of 2292 and 2363 nm was 750 mW. According to spectral intensity distribution, the output powers of 2363 and 2292 nm were estimated to be 340 and 410 mW, respectively. The saturation of output power was not observed. In this experiment, we found that the output power at 2292 nm increased more rapidly than the output power at 2363 nm when the incident pump power increased. A possible reason was that a competition existed between the two emission lines at 2292 and 2363 nm from $^3H_4$ and $^3H_5$ multiplets. Similar laser behavior also happened in the 2.3 μm Tm:Klu$(WO_4)_2$ laser[23].

The polarization states of the output laser beams were also measured by a Glan prism. The laser emissions on the $^3H_4 \rightarrow {}^3H_5$ transition at 2292 and 2363 nm were both linearly polarized along the c axis of the Tm:YVO_4 crystal ($E\|c$, π-polarization). The laser emission on the $^3H_4 \rightarrow {}^3H_5$ transition at 2108 nm was also linearly polarized and perpendicular to the c axis ($E \perp c$, σ-polarization). The polarizations were naturally selected by the anisotropy of the laser gain.

By using the knife-edge method, the output laser beam radius of Tm:YVO_4 laser as a function of the distance from a focusing

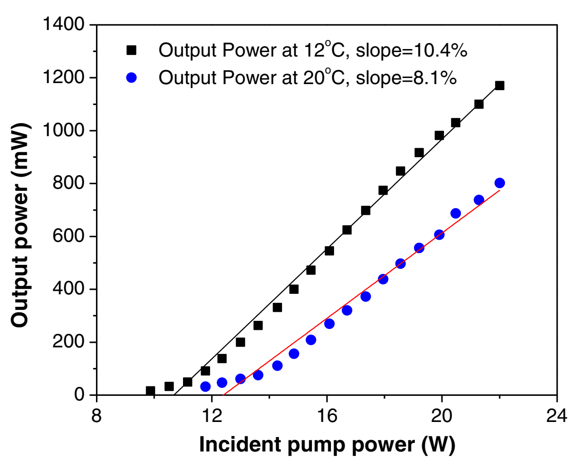

Fig. 4. Output powers versus incident pump power for the Tm:YVO_4 laser at the heat sink temperatures of 12°C and 20°C.

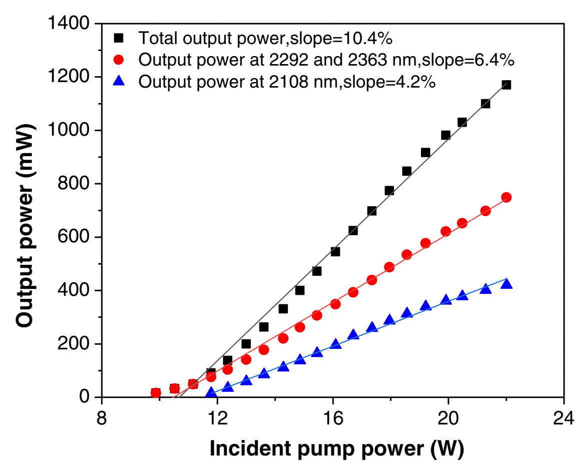

Fig. 5. Output powers versus incident pump power for the Tm:YVO_4 laser at the heat sink temperature of 12°C.

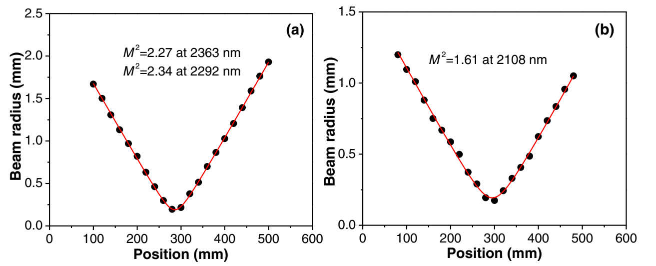

Fig. 6. Measured beam qualities of the Tm:YVO_4 laser at maximum output power: (a) M^2 = 2.34 at 2292 and M^2 = 2.27 at 2363 nm; (b) M^2 = 1.61 at 2108 nm.

lens was achieved. The focusing lens ($f = 100$ mm) was placed 160 mm away from the output coupler M2. As shown in Fig. 6, for the maximum output powers of 750 mW at 2292 and 2363 nm and 420 mW at 2108 nm, the M^2 beam quality factors were calculated to be 2.34, 2.27, and 1.61 at 2292, 2363, and 2108 nm, respectively.

For efficient laser operation at 2 μm ($^3F_4 \rightarrow {}^3H_6$), Tm^{3+} ion concentration was commonly greater than 2%. Low Tm^{3+} ion concentration (<2%) was not beneficial to improve 2 μm laser performance[22]. However, for the 1.5% Tm:YVO_4 crystal used in this experiment, laser emission at 2108 nm was realized. To further study this laser behavior, the laser emission on the $^3H_4 \rightarrow {}^3H_5$ transition was suppressed by increasing the transmittance of the output coupler in this experiment. So, the output coupler M2 was replaced by another output coupler, which was designed for partial reflection at 1900–2150 nm ($R = 95\%$) and high transmissivity at 2250–2400 nm ($T > 80\%$). Other parameters remained unchanged. With increasing incident pump power to 20 W, the laser emission on the $^3F_4 \rightarrow {}^3H_6$ transition at 1900–2150 nm was not observed. This indicated that 2.3 μm laser oscillation on the $^3H_4 \rightarrow {}^3H_5$ transition was beneficial to improve 2 μm laser operation on the $^3F_4 \rightarrow {}^3H_6$ transition, since the laser level $^3H_5$ was rapidly depopulated by multiphonon processes to the level $^3F_4$[22].

4. Conclusion

In conclusion, a Tm-doped vanadate laser operating on the $^3H_4 \rightarrow {}^3H_5$ transition was reported for the first time. For this, an a-cut Tm:YVO_4 crystal with 1.5% Tm^{3+} ion concentration was employed. Laser emissions at 2292 and 2363 nm on the $^3H_4 \rightarrow {}^3H_5$ transition and at 2108 nm on the $^3F_4 \rightarrow {}^3H_6$ transition were realized. For the pump power of 22 W, the Tm:YVO_4 laser generated a total output power of 1.17 W with a total optical-optical efficiency of 5.3% and a slope efficiency of 10.4% (versus the incident pump power). The output powers of 750 mW at π-polarized 2292 and 2363 nm and 420 mW at σ-polarized 2108 nm were simultaneously obtained. The 2.3 μm Tm:YVO_4 laser has the potential to be applied to multi-gas detection. In this experiment, only a 1% transmission output coupler at 2.3 μm was used. If the proper output coupler was used, desired output wavelengths would be obtained. Output powers and conversion efficiency would be improved by proper Tm^{3+} concentration and crystal length. The Tm:YVO_4 crystal as laser gain medium can be used in passively Q-switched regime to achieve short pulses.

Acknowledgement

This work was supported by the Fundamental Research Funds for the Central Universities and the National Natural Science Foundation of China (No. 61378027).

References

1. F. J. McAleavey, J. O'Gorman, J. F. Donegan, B. D. MacCraith, J. Hegarty, and G. Mazé, "Narrow linewidth, tunable Tm^{3+}-doped fluoride fiber laser for optical-based hydrocarbon gas sensing," IEEE J. Sel. Top. Quantum Electron. **3**, 1103 (1997).
2. A. Garnache, A. Liu, L. Cerutti, and A. Campargue, "Intracavity laser absorption spectroscopy with a vertical external cavity surface emitting laser at 2.3 μm: application to water and carbon dioxide," Chem. Phys. Lett. **416**, 22 (2005).
3. J. T. Olesberg, M. A. Arnold, C. Mermelstein, J. Schmitz, and J. Wagner, "Tunable laser diode system for noninvasive blood glucose measurements," Appl. Spectrosc. **59**, 1480 (2005).
4. S. T. Fard, W. Hofmann, P. T. Fard, G. Bohm, M. Ortsiefer, E. Kwok, M.-C. Amann, and L. Chrostowski, "Optical absorption glucose measurements using 2.3 μm vertical-cavity semiconductor lasers," IEEE Photon. Technol. Lett. **20**, 930 (2008).
5. J. Zhao, Y. Li, S. Zhang, L. Li, and X. Zhang, "Diode-pumped actively Q-switched Tm:YAP/$BaWO_4$ intracavity Raman laser," Opt. Express **23**, 10075 (2015).
6. R. Wang, S. Sprengel, G. Boehm, M. Muneeb, R. Baets, M. Amann, and G. Roelkens, "2.3 μm range InP-based type-II quantum well Fabry-Perot lasers heterogeneously integrated on a silicon photonic integrated circuit," Opt. Express **24**, 21081 (2016).
7. S. Vasilyev, I. Moskalev, M. Mirov, S. Mirov, and V. Gapontsev, "Multi-watt mid-IR femtosecond polycrystalline Cr^{2+}:ZnS and Cr^{2+}:ZnSe laser amplifiers with the spectrum spanning 2.0–2.6 μm," Opt. Express **24**, 1616 (2016).
8. U. Demirbas and A. Sennaroglu, "Intracavity-pumped Cr^{2+}:ZnSe laser with ultrabroad tuning range between 1880 and 3100 nm," Opt. Lett. **31**, 2293 (2006).
9. J. A. Caird, L. G. DeShazer, and J. Nella, "Characteristics of room temperature 2.3-μm laser emission from Tm^{3+} in YAG and $YAlO_3$," IEEE J. Quantum Electron. **11**, 874 (1975).
10. L. Guillemot, P. Loiko, E. Kifle, J.-L. Doualan, A. Braud, F. Starecki, T. Georges, J. Rouvillain, A. Hideur, and P. Camy, "Watt-level midinfrared continuous-wave Tm:YAG laser operating on the $^3H_4 \rightarrow {}^3H_5$ transition," Opt. Mater. **101**, 109745 (2020).
11. L. Guillemot, P. Loiko, A. Braud, J.-L. Doualan, A. Hideur, M. Koselja, R. Moncorgé, and P. Camy, "Continuous-wave Tm:$YAlO_3$ laser at ∼2.3 μm," Opt. Lett. **44**, 5077 (2019).
12. F. Wang, H. Huang, F. Wu, H. Chen, Y. Bao, Z. Li, O. L. Antipov, S. S. Balabanov, and D. Shen, "2.3–2.5 μm laser operation of LD-pumped Tm:YAP on the $^3H_4 \rightarrow {}^3H_5$ transition," Opt. Mater. **115**, 111054 (2021).
13. E. Kifle, P. Loiko, L. Guillemot, J. Doualan, F. Starecki, A. Braud, T. Georges, J. Rouvillain, and P. Camy, "Watt-level diode-pumped thulium lasers around 2.3 μm," Appl. Opt. **59**, 7530 (2020).
14. L. Dong, H. Chu, S. Xu, S. Zhao, and D. Li, "Sulfur-doped graphitic carbon nitride for Tm:$YAlO_3$ laser operation at 2.3 μm," Opt. Lett. **46**, 2043 (2021).
15. J. F. Pinto, L. Esterowitz, and G. H. Rosenblatt, "Tm^{3+}:YLF laser continuously tunable between 2.20 and 2.46 μm," Opt. Lett. **19**, 883 (1994).
16. I. Yorulmaz and A. Sennaroglu, "Low-threshold diode-pumped 2.3-μm Tm^{3+}:YLF Lasers," IEEE J. Sel. Top. Quantum Electron. **24**, 1601007 (2018).
17. H. Huang, S. Wang, H. Chen, O. L. Antipov, S. S. Balabanov, and D. Shen, "High power simultaneous dual-wavelength CW and passively-Q-switched

laser operation of LD pumped Tm:YLF at 1.9 and 2.3 μm," Opt. Express **27**, 38593 (2019).
18. F. Canbaz, I. Yorulmaz, and A. Sennaroglu, "Kerr-lens mode-locked 2.3-μm Tm^{3+}:YLF laser as a source of femtosecond pulses in the mid-infrared," Opt. Lett. **42**, 3964 (2017).
19. A. Muti, M. Tonelli, V. Petrov, and A. Sennaroglu, "Continuous-wave mid-infrared laser operation of Tm^{3+}:KY_3F_{10} at 2.3 μm," Opt. Lett. **44**, 3242 (2019).
20. L. Guillemot, P. Loiko, R. Soulard, A. Braud, J. Doualan, A. Hideur, and P. Camy, "Close look on cubic Tm:KY_3F_{10} crystal for highly efficient lasing on the $^3H_4 \rightarrow {}^3H_5$transition," Opt. Express **28**, 3451 (2020).
21. A. Muti, F. Canbaz, M. Tonelli, J. E. Bae, F. Rotermund, V. Petrov, and A. Sennaroglu, "Graphene mode-locked operation of Tm^{3+}:$YLiF_4$ and Tm^{3+}:KY_3F^{10} lasers near 2.3 μm," Opt. Lett. **45**, 656 (2020).
22. V. Sudesh and J. A. Piper, "Spectroscopy, modeling, and laser operation of thulium-doped crystals at 2.3 μm," IEEE J. Quantum Electron. **36**, 879 (2000).
23. P. Loiko, E. Kifle, L. Guillemot, J. Doualan, F. Starecki, A. Braud, M. Aguiló, F. Díaz, V. Petrov, X. R. Mateos, and P. Camy, "Highly efficient 2.3 μm thulium lasers based on a high-phonon-energy crystal: evidence of vibronic-assisted emissions," J. Opt. Soc. Am. B **38**, 482 (2021).
24. P. Loiko, R. Soulard, L. Guillemot, G. Brasse, J. L. Doualan, A. Braud, A. Tyazhev, A. Hideur, F. Druon, and P. Camy, "Efficient Tm:$LiYF_4$ Lasers at ∼2.3 μm: effect of energy-transfer upconversion," IEEE J. Quantum Electron. **55**, 1700212 (2019).
25. H. Hu, H. Huang, J. Huang, J. Deng, W. Weng, J. Li, and W. Lin, "Watt-level passively *Q*-switched Tm:YVO_4 laser with few-layer WSe_2 saturable absorber," Infrared Phys. Technol. **113**, 103554 (2021).
26. H. Saito, S. Chaddha, R. S. E. Chang, and N. Djeu, "Efficient 1.94-μm Tm^{3+} laser in YVO_4 host," Opt. Lett. **17**, 189 (1992).
27. R. Lisiecki, P. Solarz, G. Dominiak-Dzik, W. Ryba-Romanowski, and T. Lukasiewicz, "Effect of temperature on spectroscopic features relevant to laser performance of YVO_4:Tm^{3+}, $GdVO_4$:Tm^{3+}, and $LuVO_4$:Tm^{3+} crystals," Opt. Lett. **35**, 3940 (2010).
28. J. Šulc, P. Koranda, P. L. Černý, H. Jelínková, Y. Urata, M. Higuchi, W. Ryba-Romanowski, R. Lisiecki, P. Solarz, G. Dominiak-Dzik, and M. Sobczyk, "Tunable lasers based on diode pumped Tm-doped vanadates Tm:YVO_4, Tm:$GdVO_4$, and Tm:$LuVO_4$," Proc. SPIE **6871**, 68711V (2008).
29. Y. Urata and S. Wada, "808-nm diode-pumped continuous-wave Tm:$GdVO_4$ laser at room temperature," Appl. Opt. **44**, 3087 (2005).
30. R. Lisiecki, P. Solarz, G. Dominiak-Dzik, W. Ryba-Romanowski, M. Sobczyk, P. Černý, J. Šulc, H. Jelínková, Y. Urata, and M. Higuchi, "Comparative optical study of thulium-doped YVO_4, $GdVO_4$, and $LuVO_4$ single crystals," Phys. Rev. B **74**, 035103 (2006).
31. J. J. Zayhowski, J. Harrison, C. Dill, III, and J. Ochoa, "Tm:YVO_4 microchip laser," Appl. Opt. **34**, 435 (1995).